JOURNAL OF GUIDANCE, CONTROL, AND DYNAMICS
Vol. 23, No. 6, November–December 2000

Decentralized Design for Integrated Flight/Propulsion Control of Aircraft

Zhenyang Chen* and Petros G. Voulgaris†
University of Illinois at Urbana–Champaign, Urbana, Illinois 61801

A direct decentralized approach to the design of integrated flight/propulsion control (IFPC) systems is considered to reduce complexity and validation drawbacks of centralized designs. The imposed triangular decentralized structure on the IFPC controller allows for separate evaluation of the engine controller as well as for the evaluation of the achievable performance of the overall IFPC system. $\mathcal{H}_\infty$ techniques that require the solution to a Riccati-like equation are used to develop the design method. This method is applied to an aircraft aeropropulsive model, and the results indicate that the approach may be a vital alternative to other techniques appearing in the literature.

I. Introduction

FUTURE military fighter design aims toward aircraft with enhanced maneuver capabilities such as high-angle-of-attack operation and short takeoff and vertical landing. To achieve these enhanced maneuvering capabilities, the propulsion system can be used to provide additional moments and forces to the ones generated primarily by the conventional aerodynamic flight control effectors. Thus, an integrated flight/propulsion control (IFPC) system is needed to coordinate the functions of both the flight and the propulsion systems.

Design techniques for IFPC are given in Refs. 1–4, where centralized as well as hierarchical controller structures are considered. When no particular structure is imposed on the controller, the resulting centralized design may produce a relatively complicated controller that is difficult to implement and validate. Furthermore, the controller of the propulsion system cannot be tested separately, which is the responsibility of the engine manufacturer.

In Refs. 1 and 3, methods to reduce the complexity of centralized controllers resulting from linear quadratic and $\mathcal{H}_\infty$ methods are presented. The centralized controller is partitioned into what is called flight and engine subcontrollers with a specific interconnection structure. More specifically, an approximation to the centralized structure by two state-decoupled subcontrollers is attempted in Ref. 1. In Refs. 3 and 4, starting again from a centralized structure, a reduction to an airfame controller that generates all commands for the aerodynamic control surfaces as well as some commands for a propulsion subcontroller is attempted. The numerical results in Refs. 1, 3, and 4 indicate that the closed-loop performance and robustness characteristics of the centralized control system are matched to an acceptable degree by the partitioned subcontrollers. Of course, there is the tradeoff between matching and subcontroller complexity. The specific partitioning can also be interpreted as a form of a hierarchical structure.

Although these subcontrollers can be implemented separately, note that the engine subcontroller is (indirectly) affected by the airframe measured variables through the airframe controller.

In this paper, in contrast to the methods in Refs. 1, 3, and 4, we do not start our IFPC design from a centralized controller to obtain, indirectly, a partitioning to appropriate subcontrollers. Rather, we proceed with a direct decentralized approach where the intended structure of the controller is imposed from the beginning. A general framework such as the one shown in Fig. 1 is employed to address IFPC design. In Fig. 1, G represents the generalized plant that contains the flight and propulsion dynamics; K is the controller; w and u represent disturbance/commands and control inputs, respectively, with $w = (w_e^T,\ w_f^T)^T$ and $u = (u_f^T, u_e^T)^T$; $\boldsymbol{z}$ is the output vector to be controlled; and $\boldsymbol{y}$ is the measurement output vector, with $\boldsymbol{z} = (z_e^T, z_f^T)^T$ and $\boldsymbol{y} = (y_f^T, y_e^T)^T$. The subscripts f and e in the partitioning of w, u, z, and $\boldsymbol{y}$ refer to what can be classified as airframe- (flight-) and propulsion-related variables, respectively. Note that the generalized plant G may contain not only the flight and propulsion dynamics to be controlled, but also weighting functions that specify desired performance requirements. We consider direct decentralized control methods, where we impose, from the beginning, an (upper-) triangular structure on the IFPC controller as in Fig. 2, where the propulsion (engine) controls u_e are generated based only on the engine measured variables y_e, whereas the flight controls u_f are based on both engine and airframe measurements y_e and y_f, respectively. Accordingly, the engine controller can be identified as K_{ee}, whereas the flight controller is identified as $K_f = (K_{ff}\ \ K_{fe})$. Although other types of decentralized structures can also be considered, the one chosen represents a well-separated propulsion subsystem that can be analyzed and tested. This can be realized because the effect of the flight controls, which are typically deflections of force and moment generating surfaces on the airframe, is quite small on the engine dynamics. Hence, there is a natural separation of an engine subsystem that is affected only by the engine controls u_e (and not by u_f) that is, the engine related variables y_e for all practical purposes depend on u_e only (whereas y_f depends on both u_f and u_e). By imposing the constraint of an upper-triangular structure on the controller K (i.e., by forcing u_e to depend only on y_e), we isolate the engine loop from the overall system. This loop consists of the engine dynamics (which is practically not affected by the airframe controls u_f) and the controller K_{ee}. It is this loop that can be tested and analyzed separately. Specifically, this structure allows us to investigate the following: What are the conditions under which there exists an engine controller K_{ee} such that, when tested only with the propulsion system, it delivers a guaranteed performance level γ in the engine-related closed-loop from w_e to z_e, whereas, when put in the IFPC framework of Fig. 2, it allows for the design of a flight controller $K_f = (K_{ff}\ \ K_{fe})$ so that the integrated closed-loop from w to z has no worse performance level than γ?

Classifying control input or output variables as engine- or flight-related may be performed in different ways. There is always a sort of natural classification, but from the controls point of our approach it may not be always desirable. Rather, an open-loop control effectiveness of the integrated system may be more appropriate to dictate how to classify a control input. If, for example, an input has a significant effect on both the engine and airframe dynamics, it may

Received 22 October 1998; revision received 17 February 1999; accepted for publication 8 January 2000.

*Research Assistant, Department of Mechanical and Industrial Engineering, 140 MEB, 1206 W. Green Street; z-chen8@students.uiuc.edu.

†Associate Professor, Department of Aeronautical and Astronautical Engineering and Coordinated Science Laboratory, 1308 W. Main Street; petros@ktisivios.csl.uiuc.edu.

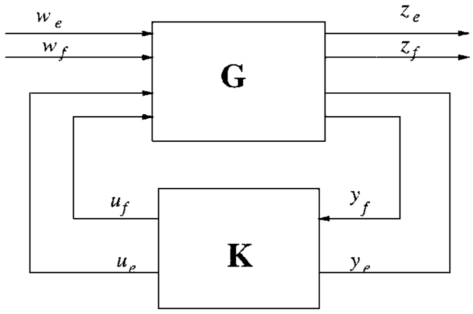

Fig. 1 Generalized plant and controller.

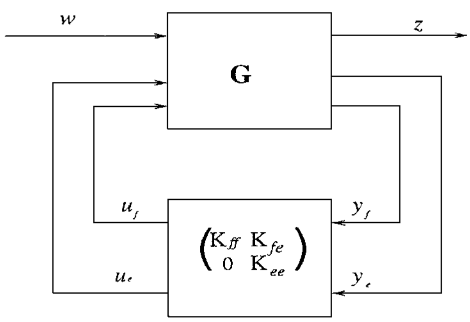

Fig. 2 Generalized plant and the decentralized controller with triangular structure.

be preferable to classify it as a flight control input, although it may seem more natural to consider it an engine variable. This is because classifying such an input as an engine variable and restricting it (by our upper-triangular scheme) to depend only on y_e may limit its effectiveness in the overall IFPC system. In the cases where there is a relatively significant effect of the control inputs u_f to the engine variables y_e (i.e., when there is a strong two-way coupling between what is considered the engine and the flight dynamics), the separation and isolation of an engine closed-loop subsystem becomes less transparent. Nonetheless, the proposed decentralized structure still provides a separated engine controller (but not necessarily a separated engine loop) that operates only on engine variables to generate engine controls.

Note that the proposed procedure is not a sequential design. That is, we do not design K_{ee} first and then, after we close the engine loop, design K_f. In a sequencial design, we may come up with a K_{ee} that works very well with the engine alone, but once hooked into the engine loop we have no guarantees that a K_f can be designed so that the overall performance in the integrated system is acceptable. In our approach we find a priori a guaranteed performance level for both the engine and the integrated system; we also furnish a K_{ee} and a K_f that deliver the guaranteed performance simultaneously.

In the paper we consider performance in terms of the $\mathcal{H}_\infty$ norm of the closed loop. The approach is based on the connection between control with a guaranteed $\mathcal{H}_\infty$ performance level and algebraic Riccati-like equations that together satisfy the decentralized structure. Based on the work in Refs. 5 and 6, a method is given on how to construct the decentralized IFPC controllers of Fig. 2 to guarantee a desirable level of performance. This method is applied to the aircraft aeropropulsive model of Ref. 1, and the results are evaluated.

II. Mathematical Preliminaries

Consider the output feedback $\mathcal{H}_\infty$-norm-bounding disturbance-rejection problem for the following linear, time-invariant system:

$$\dot{x} = Ax + Bu + Gw_0, \qquad y = Cx + Du + n, \qquad z = \begin{pmatrix} Hx \\ u \end{pmatrix} \tag{1}$$

where w_0 and n are exogenous inputs such as disturbances and/or commands and sensor noise, z is the output to be regulated, y is the measurement, and u is the control input.

There is a vast literature on methods for $\mathcal{H}_\infty$-norm-bounding controller design that rely on the solutions of algebraic Riccati equations (e.g., Chapters 15 and 16 in Ref. 7 and references therein) or, more recently, on the solution of linear matrix inequalities (LMIs).[8–10] When structural constraints on the controller are imposed (e.g., reduced order, decentralization, etc.) the optimal $\mathcal{H}_\infty$ problem becomes hard to solve. Nonetheless, several methods for practical design have been proposed with either Riccati (Refs. 5 and 6, Chapter 20 in Ref. 7) or LMI-based[11] methods.

Our approach to derive an $\mathcal{H}_\infty$-norm-bounding controller is based on the algebraic Riccati equation (ARE) methods as used in Refs. 5, 6, and 12. In particular, given a specified controller structure, obtain the closed-loop system with state-space description

$$\dot{x}_a = F_a x_a + G_a w, \qquad z = H_a x_a \tag{2}$$

where $w = (w_0^T, n^T)^T$. Then select, if possible, controller parameters so that the ARE

$$F_a^T P_a + P_a F_a + (1/\gamma^2) P_a G_a G_a^T P_a + H_a^T H_a = 0$$

has a solution $P_a \geq 0$. If (F_a, H_a) is a detectable pair, then the closed-loop system (2) is stable, and the closed-loop transfer function matrix $T(s) = H_a(sI - F_a)^{-1} G_a$ from w to z satisfies $\|T\|_\infty < \gamma$.

The idea of designing a decentralized control system with certain structure stems from the aforementioned approach. First fix the controller structure in the desired upper- (or lower-) triangular form, then select, if possible, the controller parameters to satisfy the resulting AREs.

For the IFPC designs, rewrite the LTI system (1) with

$$\dot{x} = Ax + (B_f \quad B_e) \begin{pmatrix} \boldsymbol{u}_f \\ \boldsymbol{u}_e \end{pmatrix} + G \begin{pmatrix} \boldsymbol{w}_{0f} \\ \boldsymbol{w}_{0e} \end{pmatrix}$$

$$\boldsymbol{y} = \begin{pmatrix} \boldsymbol{y}_f \\ \boldsymbol{y}_e \end{pmatrix} = \begin{pmatrix} C_f \\ C_e \end{pmatrix} x + \begin{pmatrix} \boldsymbol{n}_f \\ \boldsymbol{n}_e \end{pmatrix}, \qquad z = \begin{pmatrix} Hx \\ \boldsymbol{u}_f \\ \boldsymbol{u}_e \end{pmatrix}, \qquad w = \begin{pmatrix} \boldsymbol{w}_0 \\ \boldsymbol{n}_f \\ \boldsymbol{n}_e \end{pmatrix}$$

Here, $\boldsymbol{y}_f$, $\boldsymbol{y}_e$, $\boldsymbol{u}_f$, $\boldsymbol{u}_e$, $\boldsymbol{n}_f$, $\boldsymbol{n}_e$, $\boldsymbol{w}_{0f}$, and $\boldsymbol{w}_{0e}$ and B_f, B_e, C_f, and C_e are vectors and matrices respectively, with appropriately matched dimensions. The subscripts e and f denote the vector or matrix being related to either the engine or the flight variables.

Denoting

$$S_f = B_f B_f^T, \qquad S_e = B_e B_e^T, \qquad S = S_f + S_e$$

$$P_c = \begin{pmatrix} P & 0 \\ 0 & P \end{pmatrix}, \qquad B_c = \begin{pmatrix} B_f & 0 \\ 0 & B_e \end{pmatrix}, \qquad I_c = \begin{pmatrix} I \\ I \end{pmatrix}$$

$$G_c = \begin{pmatrix} G \\ G \end{pmatrix}, \qquad C_c = \begin{pmatrix} C_f & 0 \\ 0 & C_e \end{pmatrix}$$

$$A_c = \begin{pmatrix} A - S_e P + (1/\gamma^2) G G^T P & S_e P \\ S_f P & A - S_f P + (1/\gamma^2) G G^T P \end{pmatrix}$$

where $P \geq 0$ solves the ARE

$$A^T P + PA + (1/\gamma^2) P G G^T P - PSP + H^T H = 0 \tag{3}$$

the following theorem is used to guide the design of the decentralized controller with upper-triangular structure.

Theorem: Let (A, H) be a detectable pair and γ be a positive scalar. Suppose $P \geq 0$ satisfies Eq. (3), $A_\gamma \equiv A + \gamma^{-2} G G^T P - SP$ is Hurwitz, and $A_\gamma + SP$ has no $j\omega$-axis eigenvalues. Let $W > 0$ satisfy the Riccati-like algebraic equation

$$A_c W + W A_c^T + (1/\gamma^2) W P_c B_c B_c^T P_c W + G_c G_c^T - W C_c^T C_c W + (W_u - W) C_c^T C_c (W_u - W)^T = 0 \tag{4}$$

with W_u in upper-triangular form, and W_u being the upper-triangular part of W. If an observer gain

$$L_c = \begin{pmatrix} L_{ff} & L_{ef} \\ 0 & L_{ee} \end{pmatrix}$$

is chosen by $L_c = W_u C_c^T$, then the decentralized feedback control law with upper-triangular structure

$$\dot{\xi}_f = \left[A - SP + (1/\gamma^2)GG^T P - L_{ff} C_f\right]\xi_f - L_{ef} C_e \xi_e + (L_{ff} \quad L_{ef}) \begin{pmatrix} \boldsymbol{y}_f \\ \boldsymbol{y}_e \end{pmatrix}$$

$$\dot{\xi}_e = \left[A - SP + (1/\gamma^2)GG^T P - L_{ee} C_e\right]\xi_e + L_{ee}\boldsymbol{y}_e$$

$$\begin{pmatrix} \boldsymbol{u}_f \\ \boldsymbol{u}_e \end{pmatrix} = \begin{pmatrix} -B_f^T P \xi_f \\ -B_e^T P \xi_e \end{pmatrix} \tag{5}$$

stabilizes plant (1), with the closed-loop transfer-function matrix of Eq. (2)

$$T(s) = H_a(sI - F_a)^{-1} G_a$$

from w to z satisfying

$$\|T\|_\infty \leq \gamma$$

□

The preceding theorem can be proven along the lines of Refs. 5 and 6, where a fully decentralized structure, that is diagonal, is imposed on the controller and a Riccati-like equation similar to Eq. (4) appears. For completeness, to account for the necessary modifications of the approach in Refs. 5 and 6, due to our current triangular structure, a proof is given in the Appendix.

The Riccati-like algebraic equation of the preceding theorem is solved by iterations. For the decentralized control system with triangular structure, the matrix W is calculated by the following steps: Compute an approximation of W_0 by first ignoring the term $Q = (W_u - W)C_c^T C_c(W_u - W)$ in Eq. (4). Then use W_0 to compute an approximation of Q_0 of Q, and use Q_0 in the obvious way to compute the next approximate solution of W_1. Iterate this procedure until the candidate solution W_i makes the matrix norm of left-hand side of Eq. (4) less than some acceptable tolerance, then take W_i as the solution of W of Eq. (4). Computational experience shows that this iteration scheme works well for small-sized problems, typically four or five state systems. For a such problems, the required time (at least for the academic examples the authors considered) was 2–3 min computation on a out-of-date 40-MHz, 64-MB Spark 2 connected to a Sun network. For larger problems, the procedure can consume a significant amount of computer time. In particular, for the problem at hand (nine states), an excess of 2 h in computation time was not unusual. Nonetheless, with a more up-to-date, stand-alone computer the computation time can be significantly reduced, at least by a factor of 4. In addition, a more sophisticated iteration scheme can also improve the computational time. This is a subject of future research that the authors plan to investigate. Once W is computed, the controller is readily obtained by Eq. (5) of the preceding theorem.

III. IFPC Design Example

A. Aircraft Model Description

The aircraft model studied here is taken from Ref. 1. It is a two-spool turbofan-engine powered aircraft with two-dimensional thrust vectoring and reversing nozzle. We consider, as in Ref. 1, only the longitudinal dynamics and, hence, a single-dimensional thrust vectoring (pitch) capability. The system dynamics are linearized at the short takeoff and landing approach-to-landing task condition, the airspeed is $V_0 = 120$ kn and the flight-path angle is $\gamma = -3$ deg. The integrated airframe and propulsion system state-space representation has the following form:

$$\dot{\boldsymbol{x}}_p = A_p \boldsymbol{x}_p + B_p \boldsymbol{u}_p, \qquad \boldsymbol{y}_p = C_p \boldsymbol{x}_p + D_p \boldsymbol{u}_p$$

where the state vector is

$$\boldsymbol{x}_p = (u \quad w \quad q \quad \theta \quad h \quad N2 \quad N25 \quad P6 \quad T41B)^T$$

with

u	= aircraft body axis forward velocity, ft/s
w	= aircraft body axis vertical velocity, ft/s
q	= aircraft pitch rate, deg/s
θ	= pitch angle, deg
h	= altitude, ft
$N2$	= engine fan speed, rpm
$N25$	= core compressor speed, rpm
$P6$	= engine mixing plane pressure, psia
$T41B$	= engine high-pressure turbine blade temperature, °R

and the control input vector is

$$\boldsymbol{u}_p = (WF \quad A78 \quad A8 \quad \delta_{\mathrm{TV}})^T$$

with

WF	= engine main burner fuel flow rate, lb/h
$A78$	= thrust reverser port area, in.^{2}
$A8$	= main nozzle throat area, in.^{2}
δ_{TV}	= nozzle thrust vectoring angle, deg

The airframe and engine output vector is

$$\boldsymbol{y}_p = (V \quad q_v \quad N2P \quad \mathrm{EPR})^T$$

with

V	= aircraft airspeed, ft/s
q_v	= pitch variable, $q + 0.1\theta$
$N2P$	= engine fan speed $N2$ as % of the maximum allowable revolutions per minute at operating condition
EPR	= engine pressure ratio

Looking at the measurement vector $\boldsymbol{y}_p$, one can naturally consider the measurements V and q_v as flight-related outputs and $N2P$ and EPR as engine related. The control inputs WF, $A78$, and $A8$ affect both the airframe (primarily the speed V) and the engine dynamics, whereas the thrust vectoring δ_{TV} has very little effect on the propulsion system dynamics. Thus, δ_{TV} can be considered as a purely flight control input. Also, the inputs $A78$ and $A8$ appear to have less impact on the flight-related outputs than WF. Hence, one can classify them as engine-related inputs. WF can be considered as an engine- or flight-related variable due to its effect on both. If WF is considered an engine-related input, it is bound to provide poor performance in our decentralized scheme; thus, it will depend only on the engine-related outputs $N2P$ and EPR and not on any of the flight variables V and q_v. This restriction can cause severe flight performance degradation, particularly in controlling the speed V. Initial decentralized designs we performed exhibited very poor performance when WF was selected as an engine input together

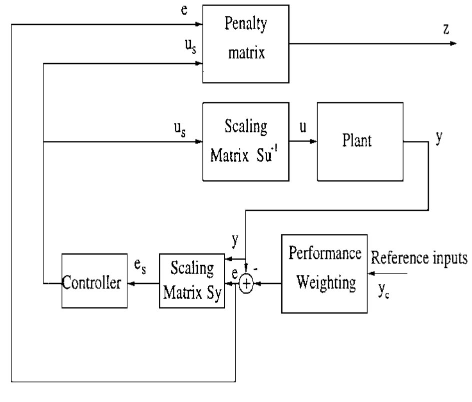

Fig. 3 Block diagram for controller designs.

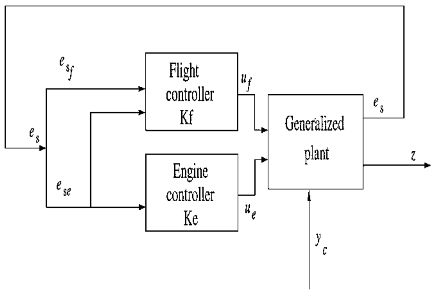

Fig. 4 System with decentralized controller in upper-triangular structure.

with $A78$ and $A8$, leaving δ_{TV} as the only flight control input. Based on this analysis, the following classification was used:

$$u_f = \begin{pmatrix} WF \\ \delta_{TV} \end{pmatrix}, \qquad u_e = \begin{pmatrix} A78 \\ A8 \end{pmatrix}$$

$$y_f = \begin{pmatrix} V \\ q_v \end{pmatrix}, \qquad y_e = \begin{pmatrix} N2P \\ \mathrm{EPR} \end{pmatrix}$$

B. Design Description and Evaluation

Both the centralized and direct partial decentralized controller designs were performed according to the framework of the block diagram in Fig. 3. In this configuration, the block plant represents

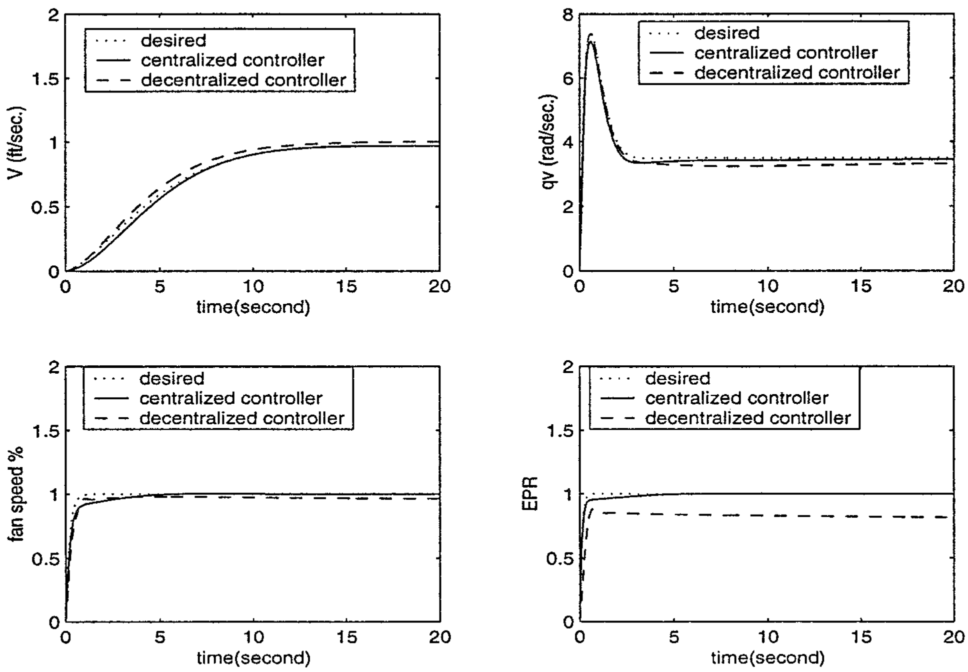

Fig. 5 Responses of V, q_v, $N2P$, and EPR to step commands V_c, δ_{st}, $N2P_c$, and EPR_c, respectively.

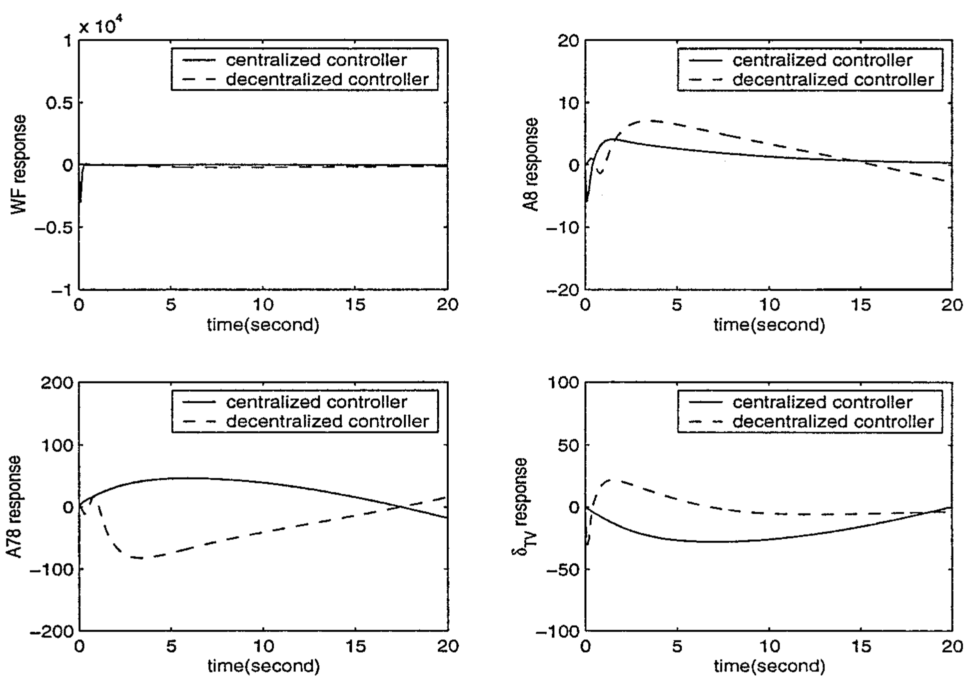

Fig. 6 Responses of controls WF in pounds per hour, $A8$ and $A78$ in inches squared, and δ_{TV} in degrees to a step input δ_{st} in inches.

the original aircraft model and the block performance weighting models the ideal command tracking properties, that is, flying quality models. These ideal models are as in Ref. 1 and are given here in the Appendix. Two scaling blocks S_u^{-1} and S_y as in Ref. 1 are used to properly scale the system to guarantee the numerical precision in the design process; these are also given in the Appendix. The controlled output of interest is z, which is composed of the weighted tracking errors e and scaled control inputs $\boldsymbol{u}_s$. The weighing occurs in the penalty matrix, where we penalize steady-state tracking errors and control action with integratorlike and constant penalties, respectively. The parameters of these type of penalties are tuned so that the good tracking performance is achieved with reasonable control energy. The controller operates on the (scaled) errors and measurement e_s and is designed to be an $\mathcal{H}_\infty$-optimal full-block controller in the centralized design and a block upper-triangular $\mathcal{H}_\infty$-norm-bounded suboptimal controller in the direct decentralized design approach.

In the direct decentralized approach, as shown in Fig. 4, the controller is designed to be in an upper-triangular structure, with the engine and flight output measurements together being used to design the flight subcontroller K_f, whereas only the engine output measurements being used to design the propulsion (engine) subcontroller K_e. All of the blocks in Fig. 3 excluding the controller block are integrated into the generalized plant in Fig. 4.

Figure 5 shows the centralized and decentralized closed-loop system response to various step command inputs V_c, δ_{st}, $N2P_c$, and EPR_c individually, where δ_{st} is the pilot stick input in inches. The dashed lines are the actual responses to the step inputs, and the solid lines are the desired responses related to the weight discussion. As can be seen from Fig. 5, the output response characteristics of the centralized design match well with the desired behavior. Moreover, the decentralized design matches fairly well with the desired response for the (flight) commands V_c and δ_{st}, whereas it exhibits a slightly inferior steady-state behavior to (engine) commands $N2P_c$ and EPR_c. This should not come as a surprise because in the decentralized design the engine controls $A8$ and $A78$ utilize

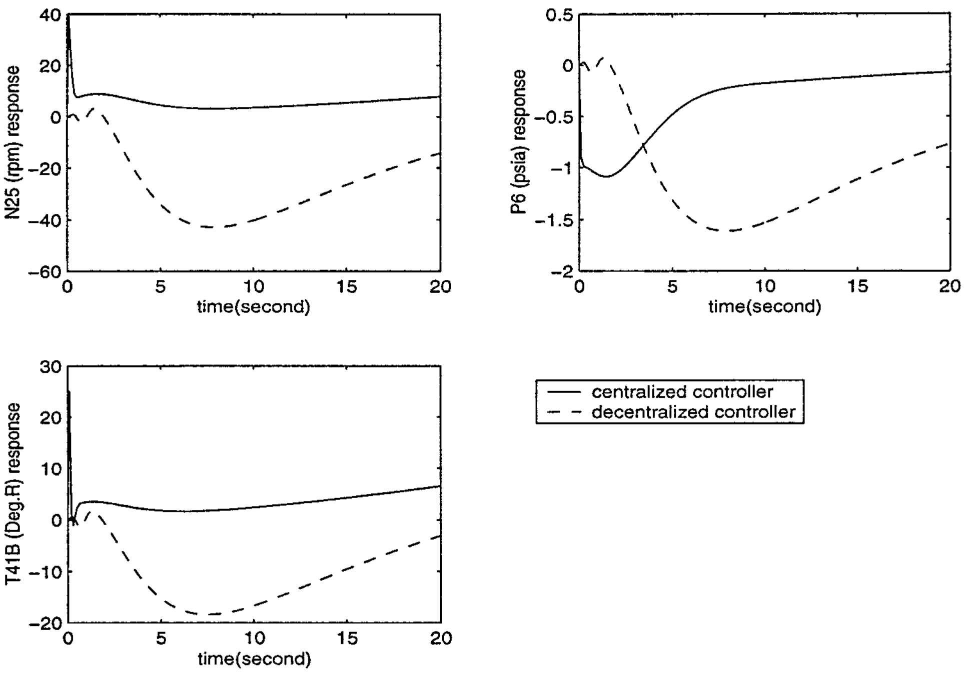

Fig. 7 Responses of $N25$, $P6$, and $T41B$ to a step input δ_{st}.

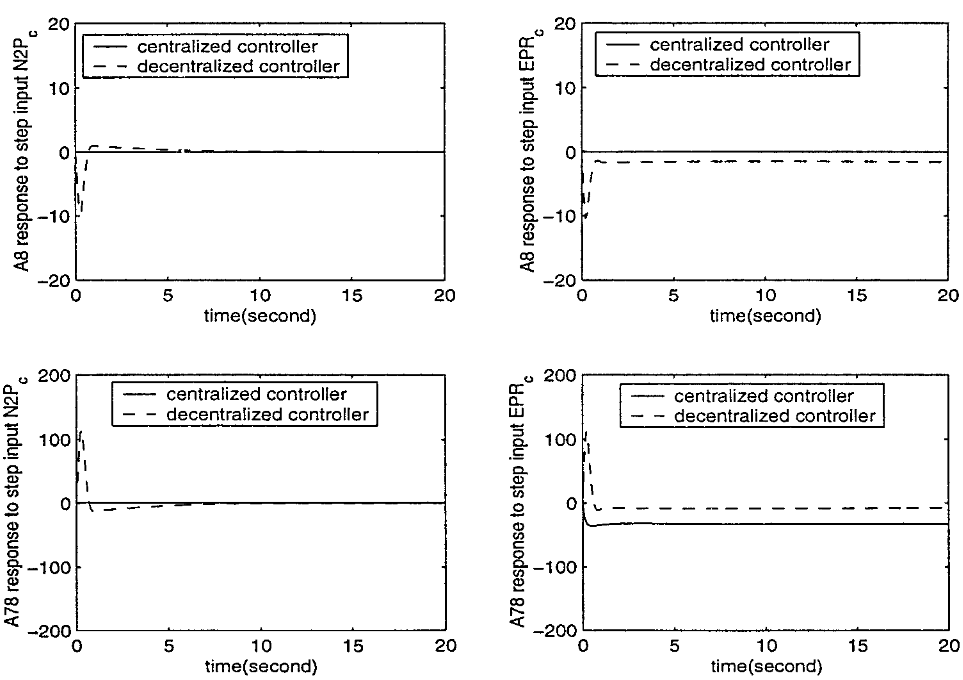

Fig. 8 Responses of $A78$ and $A8$ in inches squared to a step input $N2P_c$ and EPR_c.

a restricted set of information as opposed to the remaining flight controls.

In all of the step responses shown the control inputs were within their maximum limits in both the centralized and decentralized designs. Also, the fan speed excursions were within operational range, although no direct limiting for surge or stall was imposed in this preliminary study. The response of the controls to a step command δ_{st} is shown in Fig. 6. The states $N25$, $P6$, and $T41B$ responses to step input δ_{st} are also shown in Fig. 7. Note that the response of the controls and the states is quite different between decentralized and centralized design despite that the outputs in Fig. 5 look similar. The difference can be noticed in both the initial as well as the steady part of the response. Generally speaking, and this holds true for all of the responses, including the ones not shown here, in the decentralized design it takes relatively longer for the states to settle. However, the decentralized response appears smoother. This also should not be a surprise. The centralized design is a more aggressive design because it utilizes all of the information and generates a faster system. Also, generally speaking, the substantially different control usage between centralized and decentralized design occurs in the response of $A8$ and $A78$ to the (engine) commands $N2P_c$ and to EPR_c. This is shown in Fig. 8, where in the decentralized design, to account for the limited information given, both $A8$ and $A78$ have to work considerably harder relative to the centralized design.

IV. Conclusion

In this paper direct decentralized $\mathcal{H}_\infty$ design of IFPC systems is studied. The approach is based on the solution to a Riccati-like equation. This equation can be quite complex to solve, which generates a need for computationally efficient methods. However, our experience with relatively simple iterative methods to solve this equation has shown that for relatively small-order systems, one can get reasonable convergence without requiring unrealistic computer time. Moreover, the results from the application of this method to an aeropropulsive model are promising, and, thus, the method may be a vital alternative to other techniques appearing in the literature.

Appendix: Proofs and Ideal Models

A. Proof of Theorem

Theorem: Let (A, H) be a detectable pair and γ be a positive scalar. Suppose $P \geq 0$ satisfies Eq. (3), $A_\gamma \equiv A + \gamma^{-2}GG^TP - SP$ is Hurwitz, and $A_\gamma + SP$ has no $j\omega$-axis eigenvalues. Let $W > 0$ satisfy the Riccati-like algebraic equation

$$A_cW + WA_c^T + (1/\gamma^2)WP_cB_cB_c^TP_cW + G_cG_c^T - WC_c^TC_cW + (W_u - W)C_c^TC_c(W_u - W)^T = 0 \tag{A1}$$

with W_u in upper-triangular form and W_u being the upper-triangular part of W. If an observer gain

$$L_c = \begin{pmatrix} L_{ff} & L_{ef} \\ 0 & L_{ee} \end{pmatrix}$$

is chosen by $L_c = W_uC_c^T$, then the decentralized feedback control law with upper-triangular structure

$$\dot{\xi}_f = [A - SP + (1/\gamma^2)GG^TP - L_{ff}C_f]\xi_f - L_{ef}C_e\xi_e + (L_{ff} \quad L_{ef})\begin{pmatrix} y_f \\ y_e \end{pmatrix}$$

$$\dot{\xi}_e = \left[A - SP + (1/\gamma^2)GG^TP - L_{ee}C_e\right]\xi_e + L_{ee}y_e$$

$$\begin{pmatrix} \boldsymbol{u}_f \\ \boldsymbol{u}_e \end{pmatrix} = \begin{pmatrix} -B_f^TP\xi_f \\ -B_e^TP\xi_e \end{pmatrix}$$

stabilizes the plant (1), with the closed-loop transfer-function matrix of Eq. (2)

$$T(s) = H_a(sI - F_a)^{-1}G_a$$

from w to z satisfying

$$\|T\|_\infty \leq \gamma$$

□

Proof: Rewrite the LTI system (1), with

$$\dot{\boldsymbol{x}} = Ax + (B_f \quad B_e)\begin{pmatrix} \boldsymbol{u}_f \\ \boldsymbol{u}_e \end{pmatrix} + Gw_0 \tag{A2}$$

$$y = \begin{pmatrix} \boldsymbol{y}_f \\ \boldsymbol{y}_e \end{pmatrix} = \begin{pmatrix} C_f \\ C_e \end{pmatrix} x + \begin{pmatrix} \boldsymbol{n}_f \\ \boldsymbol{n}_e \end{pmatrix} \tag{A3}$$

$$z = \begin{pmatrix} H\boldsymbol{x} \\ \boldsymbol{u}_f \\ \boldsymbol{u}_e \end{pmatrix} \tag{A4}$$

$$w = \begin{pmatrix} w_0 \\ \boldsymbol{n}_f \\ \boldsymbol{n}_e \end{pmatrix} \tag{A5}$$

Here, $\boldsymbol{y}_f$, $\boldsymbol{y}_e$, $\boldsymbol{u}_f$, $\boldsymbol{u}_e$, $\boldsymbol{n}_f$, and $\boldsymbol{n}_e$ are vectors with appropriately matched dimensions and B_f, B_e, C_f, and C_e are matrices with appropriately matched dimensions. The subscripts e and f denote the vector or matrix being related to either the engine or the flight variables. Thus, the revised problem becomes to design a controller $u^T = (u_f^T, u_e^T)^T$, where the design of the $\boldsymbol{u}_f$ control law uses the local measurements $\boldsymbol{y}_f$ as well as the measurements $\boldsymbol{y}_e$, whereas the design of the $\boldsymbol{u}_e$ control law uses only the local measurements $\boldsymbol{y}_e$. These controllers are based on the observers that form the estimate vectors $\boldsymbol{\xi}_f$ and $\boldsymbol{\xi}_e$ of the state vectors $\boldsymbol{x}$ for feedback control. These state estimate vectors are used for feedback so as to approximate the state feedback control law.

Let $P \geq 0$ solve Eq. (3), which is the ARE related to the system (1). Then the output feedback control laws generated will be in the following form:

$$\begin{pmatrix} \boldsymbol{u}_f \\ \boldsymbol{u}_e \end{pmatrix} = \begin{pmatrix} -B_f^TP\boldsymbol{\xi}_f \\ -B_e^TP\boldsymbol{\xi}_e \end{pmatrix}$$

To best approximate the plant dynamics, the ideal form of the observer should be as follows:

$$\dot{\boldsymbol{\xi}}_f = A\boldsymbol{\xi}_f + B_f\boldsymbol{u}_f + B_e\hat{\boldsymbol{u}}_e + G\boldsymbol{n}_{of} + L_f\left[\begin{pmatrix} \boldsymbol{y}_f \\ \boldsymbol{y}_e \end{pmatrix} - \begin{pmatrix} C_f\boldsymbol{\xi}_f \\ C_e\boldsymbol{\xi}_e \end{pmatrix}\right]$$

$$\dot{\boldsymbol{\xi}}_e = A\boldsymbol{\xi}_e + B_e\boldsymbol{u}_e + B_f\hat{\boldsymbol{u}}_f + G\boldsymbol{n}_{oe} + L_e(\boldsymbol{y}_e - C_e\boldsymbol{\xi}_e)$$

where $\boldsymbol{n}_{of}$ and $\boldsymbol{n}_{oe}$ are estimates of the worst disturbances and L_f and L_e are observer gains used in designing the observers $\boldsymbol{\xi}_f$ and $\boldsymbol{\xi}_e$, respectively. The approximation of the control applied by engine or flight controller is $\hat{\boldsymbol{u}}_e$ or $\hat{\boldsymbol{u}}_f$, as seen from one another's control loop:

$$\begin{pmatrix} \boldsymbol{n}_{of} \\ \boldsymbol{n}_{oe} \end{pmatrix} = \begin{pmatrix} (1/\gamma^2)G^TP\boldsymbol{\xi}_f \\ (1/\gamma^2)G^TP\boldsymbol{\xi}_e \end{pmatrix}, \qquad \begin{pmatrix} \hat{\boldsymbol{u}}_e \\ \hat{\boldsymbol{u}}_f \end{pmatrix} = \begin{pmatrix} -B_e^TP\boldsymbol{\xi}_f \\ -B_f^TP\boldsymbol{\xi}_e \end{pmatrix}$$

Denote $L_f = (L_{ff}, L_{ef})$ and $L_e = (L_{fe}, L_{ee}) = (0, L_{ee})$, and rearrange the preceding equations (A2–A5)

$$\dot{\boldsymbol{x}} = A\boldsymbol{x} - B_fB_f^TP(\boldsymbol{x} + e_f) - B_eB_e^TP(\boldsymbol{x} + e_e) + Gw_0$$

$$\dot{e}_f = \dot{\boldsymbol{\xi}}_f - \dot{\boldsymbol{x}}$$

$$= Ae_f - B_eB_e^TP(e_f - e_e) + (1/\gamma^2)GG^TP(x + e_f) - Gw_0 + (L_{ff}, L_{ef})\begin{pmatrix} \boldsymbol{n}_f \\ \boldsymbol{n}_e \end{pmatrix} - (L_{ff}, L_{ef})\begin{pmatrix} C_fe_f \\ C_ee_e \end{pmatrix}$$

$$\dot{e}_e = \dot{\boldsymbol{\xi}}_e - \dot{\boldsymbol{x}}$$

$$= Ae_e - B_fB_f^TP(e_e - e_f) + (1/\gamma^2)GG^TP(x + e_e) - Gw_0 + L_en_e - L_eC_ee_e$$

that is,

$$\dot{\tilde{\boldsymbol{x}}}_a = \tilde{F}_a\tilde{\boldsymbol{x}}_a + \tilde{G}_a w, \qquad z = \begin{pmatrix} Hx \\ \boldsymbol{u}_f \\ \boldsymbol{u}_e \end{pmatrix} = \tilde{H}_a \boldsymbol{x}_a$$

with $\tilde{\boldsymbol{x}}_a^T = (x^T, e_f^T, e_e^T)^T$. To bound the $\mathcal{H}_\infty$ norm of the closed-loop system, there must be a $\tilde{P}_a \geq 0$ satisfying the following ARE:

$$\tilde{F}_a^T \tilde{P}_a + \tilde{P}_a \tilde{F}_a + (1/\gamma^2)\tilde{P}_a \tilde{G}_a \tilde{G}_a^T \tilde{P}_a + \tilde{H}_a^T \tilde{H}_a = 0 \tag{A6}$$

with

$$\tilde{P}_a = \begin{pmatrix} P & 0 \\ 0 & P_1 \end{pmatrix}$$

$(\tilde{F}_{a_2}\, \tilde{H}_a)$ being a detectable pair and $\tilde{F}_a$ being Hurwitz. Here, $P \geq 0$ in $\tilde{P}_a$ solves ARE (3), and $P_1 > 0$ is to be determined.

To simplify to the derivation, let us adopt the following notation:

$$S_f = B_f B_f^T, \qquad S_e = B_e B_e^T, \qquad S = S_f + S_e \tag{A7}$$

$$P_c = \begin{pmatrix} P & 0 \\ 0 & P \end{pmatrix}, \qquad B_c = \begin{pmatrix} B_f & 0 \\ 0 & B_e \end{pmatrix}, \qquad I_c = \begin{pmatrix} I_f \\ I_e \end{pmatrix} \tag{A8}$$

$$G_c = \begin{pmatrix} I_f \\ I_e \end{pmatrix} G, \qquad L_c = \begin{pmatrix} L_{ff} & L_{ef} \\ 0 & L_{ee} \end{pmatrix}, \qquad C_c = \begin{pmatrix} C_f & 0 \\ 0 & C_e \end{pmatrix} \tag{A9}$$

$$A_c = \begin{bmatrix} A - S_e P + (1/\gamma^2) G G^T P & S_e P \\ S_f P & A - S_f P + (1/\gamma^2) G G^T P \end{bmatrix} \tag{A10}$$

Thus,

$$\tilde{F}_a = \begin{bmatrix} A - SP & -BB_c^T P_c \\ (1/\gamma^2) G_c G^T P & A_c - L_c C_c \end{bmatrix}, \qquad \tilde{G}_a = \begin{pmatrix} G & 0 \\ -G_c & L_c \end{pmatrix}$$

$$\tilde{H}_a = \begin{pmatrix} H & 0 \\ -B_c^T P_c I_c & -B_c^T P_c \end{pmatrix}$$

The left-hand side of Eq. (A.6) becomes

$$\begin{aligned}
&\tilde{F}_a^T \tilde{P}_a + \tilde{P}_a \tilde{F}_a + (1/\gamma^2)\tilde{P}_a \tilde{G}_a \tilde{G}_a^T \tilde{P}_a + \tilde{H}_a^T \tilde{H}_a \\
&= \begin{pmatrix} (A - SP)^T P & \left[(1/\gamma^2) G_c G^T P\right]^T P_1 \\ \left(-BB_c^T P_c\right)^T P & (A_c - L_c C_c)^T P_1 \end{pmatrix} \\
&+ \begin{pmatrix} P(A - SP) & -PBB_c^T P_c \\ (1/\gamma^2) P_1 G_c G P & P_1 (A_c - L_c C_c) \end{pmatrix} \\
&+ \frac{1}{\gamma^2}\begin{pmatrix} PGG^T P & -PGG_c^T P_1 \\ -P_1 G_c G^T P & P_1\left(G_c G_c^T + L_c L_c^T\right) P_1 \end{pmatrix} \\
&+ \begin{bmatrix} H^T H + \left(B_c^T P_c I_c\right)^T \left(B_c^T P_c I_c\right) & \left(B_c^T P_c I_c\right)^T B_c^T P_c \\ \left(B_c^T P_c\right)^T \left(B_c^T P_c I_c\right) & \left(B_c^T P_c\right)^T \left(B_c^T P_c\right) \end{bmatrix} \\
&= \begin{pmatrix} U_{11} & U_{12} \\ U_{12}^T & U_{22} \end{pmatrix} = U
\end{aligned} \tag{A11}$$

If we can find a set of parameters to make the matrix U equal zero, the corresponding ARE (A.6) of the closed-loop system will be satisfied. Furthermore, as will be shown in the lemma, $\tilde{F}_a$ and $\tilde{H}_a$ can be proven to be a detectable pair, and $\tilde{F}_a$ is Hurwitz. Then we can draw the conclusion that the closed-loop system is stable and has a bounded $\mathcal{H}_\infty$ norm, that is, $\|\tilde{T}(s)\|_\infty < \gamma$ for all frequencies, where $\tilde{T}(s) = \tilde{H}_a(sI - \tilde{F}_a)^{-1}\tilde{G}_a$.

After rearranging the terms related to U_{11}, we find out that $U_{11} = 0$ from the ARE (3). Also, it turns out that the off-diagonal block U_{12} also equals zero.

Now Eq. (A.11) becomes

$$\tilde{F}_a^T \tilde{P}_a + \tilde{P}_a \tilde{F}_a + (1/\gamma^2)\tilde{P}_a \tilde{G}_a \tilde{G}_a^T \tilde{P}_a + \tilde{H}_a^T \tilde{H}_a = \begin{pmatrix} 0 & 0 \\ 0 & U_{22} \end{pmatrix}$$

with

$$\begin{aligned}
U_{22} &= A_c^T P_1 + P_1 A_c - C_c^T L_c^T P_1 - P_1 L_c C_c + (1/\gamma^2)\left(P_1 G_c G_c^T P_1\right. \\
&\quad \left. + P_1 L_c L_c^T P_1\right) + P_c B_c B_c^T P_c
\end{aligned}$$

However,

$$\begin{aligned}
U_{22} &= P_1\left[P_1^{-1} A_c^T + A_c P_1^{-1} - P_1^{-1} C_c^T L_c^T - L_c C_c P_1^{-1}\right. \\
&\quad \left. + (1/\gamma^2) G_c G_c^T + (1/\gamma^2) L_c L_c^T + P_1^{-1} P_c B_c B_c^T P_c P_1^{-1}\right] P_1
\end{aligned}$$

By the denoting of $W = \gamma^2 P_1^{-1}$, then $P_1^{-1} = (1/\gamma^2) W$ the preceding U_{22} related equation becomes

$$U_{22} = (1/\gamma^2) P_1 \Sigma P_1$$

with

$$\begin{aligned}
\Sigma &= W A_c^T + A_c W - W C_c^T L_c^T - L_c C_c W + G_c G_c^T + L_c L_c^T \\
&\quad + (1/\gamma^2) W P_c B_c B_c^T P_c W = A_c W + W A_c^T \\
&\quad + (1/\gamma^2) W P_c B_c B_c^T P_c W + G_c G_c^T - W C_c^T C_c W \\
&\quad + \left(L_c - W C_c^T\right)\left(L_c^T - C_c W\right)
\end{aligned}$$

Now, we can pick P_1 or, equivalently, L_c and W, to make $U_{22} = 0$. Moreover, L_c must be of block lower- or upper-triangular form. By the defining of

$$W = \begin{pmatrix} W_{11} & W_{12} \\ W_{12} & W_{22} \end{pmatrix}, \qquad W_u = \begin{pmatrix} W_{11} & W_{12} \\ 0 & W_{22} \end{pmatrix}$$

then

$$L_c = W_u C_c^T = \begin{pmatrix} L_{ff} & L_{ef} \\ 0 & L_{ee} \end{pmatrix} = \begin{pmatrix} W_{11} & W_{12} \\ 0 & W_{22} \end{pmatrix} \begin{pmatrix} C_f^T & 0 \\ 0 & C_e^T \end{pmatrix} \tag{A12}$$

thus,

$$\begin{aligned}
U_{22} &= (1/\gamma^2) P_1\left[A_c W + W A_c^T + (1/\gamma^2) W P_c B_c B_c^T P_c W + G_c G_c^T\right. \\
&\quad \left. - W C_c^T C_c W + (W_u - W) C_c^T C_c (W_u - W)^T\right] P_1
\end{aligned}$$

with U_{22} being zero is needed.

The results stipulate that a Riccati-like algebraic equation

$$\begin{aligned}
&A_c W + W A_c^T + (1/\gamma^2) W P_c B_c B_c^T P_c W + G_c G_c^T - W C_c^T C_c W \\
&\quad + (W_u - W) C_c^T C_c (W_u - W)^T = 0
\end{aligned} \tag{A13}$$

must be satisfied by carefully choosing L_c and W with $W > 0$. □

Now we need to find conditions under which $\tilde{F}_a$ and $\tilde{H}_a$ is a detectable pair.

Lemma: Given the definitions of Eqs. (A7–A10), where $P \geq 0$ satisfies Eq. (3), $W > 0$ satisfies Eq. (A13), and L_c satisfies Eq. (A12), the pair $\tilde{F}_a$ and $\tilde{H}_a$ is detectable under the following three conditions:

1) A and H is a detectable pair.
2) $A_\gamma \equiv A + (1/\gamma^2) G G^T P - SP$ is Hurwitz.
3) $A_\gamma + SP$ has no eigenvalues on the $j\omega$ axis.

Proof: Assume λ is an eigenvalue of $\tilde{F}_a$ corresponding to an unobservable mode of $\tilde{F}_a$ and $\tilde{H}_a$, that is, some $v^T = (v_1^T, v_2^T) \neq 0$ satisfies

$$\tilde{F}_a v = \begin{pmatrix} A - SP & -BB_c^T P_c \\ (1/\gamma^2) G_c G^T P & A_c - L_c C_c \end{pmatrix} \begin{pmatrix} v_1 \\ v_2 \end{pmatrix} = \lambda \begin{pmatrix} v_1 \\ v_2 \end{pmatrix} \tag{A14}$$

and

$$\tilde{H}_a v = \begin{pmatrix} H & 0 \\ -B_c^T P_c I_c & -B_c^T P_c \end{pmatrix} \begin{pmatrix} v_1 \\ v_2 \end{pmatrix} = 0 \tag{A15}$$

Now we want to show $R_e(\lambda) < 0$ so that the pair $\tilde{F}_a$ and $\tilde{H}_a$ is detectable.

From the lower block of Eq. (A15) and the upper block of Eq. (A14) we can get

$$Av_1 = \lambda v_1 \tag{A16}$$

$$Hv_1 = 0 \tag{A17}$$

Because A and H is a detectable pair from the assumption, this implies that either $R_e(\lambda) < 0$ (thus, $\tilde{F}_a$ and $\tilde{H}_a$ is detectable) or $v_1 = 0$. If $v_1 = 0$, then $(A_c - L_c C_c)v_2 = \lambda v_2$ from Eq. (A14). If $A_c - L_c C_c$ can be proven to be Hurwitz, the detectability proof is completed. From the equation related to $U_{22} = 0$, we have

$$(A_c - L_c C_c)W + W(A_c - C_c L_c)^T + (1/\gamma^2)W P_c B_c B_c^T P_c W + G_c G_c^T + L_c L_c^T = 0 \tag{A18}$$

Let η^* and η be the left and right eigenvectors of $A_c - L_c C_c$ corresponding to the eigenvalue λ, and multiply Eq. (A18) on the left by η^* and on the right by η to obtain

$$2R_e(\lambda)\eta^* W\eta + (1/\gamma^2)\eta^* W P_c B_c B_c^T P_c W\eta + \eta^* G_c G_c^T \eta + \eta^* L_c L_c^T \eta = 0 \tag{A19}$$

Because every term in Eq. (A19) is nonnegative, and $W > 0$ from assumption, from $R_e(\lambda)\eta^* W\eta \leq 0$, $R_e(\lambda) \leq 0$ is reached. However, if $R_e(\lambda) = 0$, then every term in Eq. (A19) must be zero; hence, $\eta^* L_c = 0$. Then λ is an eigenvalue of A_c. If we use a similarity transformation matrix M to transform A_c to $M^{-1}A_c M$, with

$$M = \begin{pmatrix} I & 0 \\ I & I \end{pmatrix}$$

then

$$M^{-1}A_c M = \begin{pmatrix} A_\gamma + SP & S_e P \\ 0 & A_\gamma \end{pmatrix}$$

However, A_γ is assumed Hurwitz, and $A_\gamma + SX$ is assumed have no imaginary eigenvalues, and so λ cannot the eigenvalue of A_c. Thus, $R_e(\lambda) < 0$ is reached. □

B. Ideal Models and Scaling Blocks

The desired response transfer functions are

$$\frac{V}{V_c} = \frac{0.04s + 0.125}{s^2 + 0.641s + 0.13}, \qquad \frac{q}{\delta_{st}} = \frac{35.12s + 17.56}{s^2 + 3.99s + 5.02}$$

$$N2P/N2P_c = 5/(s + 5), \qquad \mathrm{EPR}/\mathrm{EPR}_c = 10/(s + 10)$$

The scaling matrices are

$$S_u = \mathrm{diag}[2.0e - 04, 0.02, 0.01, 0.1]$$

$$S_y = \mathrm{diag}[0.05, 0.3, 0.2, 3.0]$$

Acknowledgment

The authors appreciate the support by Office of Naval Research under the Young Investigator Program Award, Grants N00014-95-0948 and N0014-97-0153.

References

[1] Garg, S., Mattern, D. L., and Bullard, R. E., "Integrated Flight/Propulsion Control System Design Based on a Centralized Approach," *Journal of Guidance, Control, and Dynamics*, Vol. 14, No. 1, 1991, pp. 107–116.

[2] Garg, S., "Robust Integrated Flight/Propulsion Control Design for a STOVL Aircraft Using H-Infinity Control Design Techniques," *Automatica*, Vol. 29, No. 1, 1993, pp. 129–145.

[3] Garg, S., "Partitioning of Centralized Integrated Flight/Propulsion Control Design for Decentralized Implementation," *IEEE Transactions on Control Systems Technology*, Vol. 1, No. 2, 1993, pp. 93–100.

[4] Schmidt, P. H., Garg, S., and Holowecky, B. R., "A Parameter Optimization Approach to Controller Partitioning for Integrated Flight/Propulsion Control Application," *IEEE Transactions on Control Systems Technology*, Vol. 1, No. 1, 1993, pp. 21–36.

[5] Veillette, R. J., Medanic, J. V., and Perkins, W. R., "Robust Stabilization and Disturbance Rejection for Uncertain Systems by Decentralized Control," *Control of Uncertain Systems*, edited by D. Hinrichsen and B. Martensson, Birkhauser, Boston, 1990, pp. 309–327.

[6] Veillette, R. J., Medanic, J. V., and Perkins, W. R., "Design of Reliable Control Systems," *IEEE Transactions on Automatic Control*, Vol. 37, No. 3, 1992, pp. 290–304.

[7] Zhou, K., Doyle, J. C., and Glover, K., *Robust and Optimal Control*, Prentice–Hall, Upper Saddle River, NJ, 1996.

[8] Gahinet, P., and Apkarian, P., "A Linear Matrix Inequality Approach to $\mathcal{H}_\infty$ Control," *International Journal of Robust and Nonlinear Control*, Vol. 4, No. 4, 1994, pp. 421–448.

[9] Boyd, S., Ghaoui, L. El., Feron, E., and Balakrishnan, V., *Linear Matrix Inequalities in Systems and Control Theory*, Society for Industrial and Applied Mathematics, Philadelphia, 1994.

[10] Iwasaki, T., and Skelton, R. E., "All Controllers for the General $\mathcal{H}_\infty$ Control Design Problem: LMI Existence Conditions and State Space Formulas," *Automatica*, Vol. 30, No. 5, 1994, pp. 1307–1317.

[11] Grigoriadis, K. M., and Skelton, R. E., "Fixed Order Control Design for LMI Control Problems Using Alternating Projection Methods," *Proceedings of the 33th IEEE Conference on Decision and Control*, 1994, pp. 2003–2008.

[12] Veillette, R. J., and Medanic, J. V., "$\mathcal{H}_\infty$-Norm Bounds for ARE-Based Design," *Systems and Control Letters*, Vol. 13, No. 3, 1989, pp. 193–204.